Supporting information

3D deterministic lateral displacement (3D-DLD) cartridge system for high throughput particle sorting

Petra Jusková, [1,2,3] Lionel Matthys, [4] Jean-Louis Viovy *[1,2,3] & Laurent Malaquin *[5]

1 Laboratoire Physico Chimie Curie, Institut Curie, PSL Research University, CNRS UMR168, 75005, Paris, France
2 Sorbonne Universités, UPMC Univ Paris 06, 75005, Paris, France
3 Institut Pierre-Gilles de Gennes, 75005, Paris, France
4 Fluigent, 67 Avenue de Fontainebleau, 94270 Le Kremlin-Bicêtre, France
5 LAAS-CNRS, Université de Toulouse, CNRS, F-31400 Toulouse, France

*Corresponding author:
Laurent Malaquin, laurent.malaquin@laas.fr
Jean-Louis Viovy, Jean-Louis.Viovy@curie.fr

Table of Contents

1. Deterministic lateral displacement: critical diameter (D_c)

The geometry and arrangement of the posts determines the value of the following the empirical equation:[1]

$$D_c = 1.4g\left(\frac{s}{g+d}\right)^{0.48} = 1.4g\left(\frac{s}{\lambda}\right)^{0.48} = 1.4g(\tan\alpha)^{0.48}$$

The array can be described by the shift (s) between subsequent rows, gap (g) between the individual posts, and the diameter of the posts (d). Centre to centre distance between two posts, equal to the sum of the gap and the post diameter is referred to as (λ). D_c depends solely on the gap between the posts and the tilt angle of the array, (α). This value is specific for every pillar arrangement. Spherical particles with a diameter < D_c will travel through the array in the direction parallel to the flow, whereas particles with a diameter D > D_c will move with the tilt angle, α and will be laterally displaced, independently of the flow rate. This equation does not take into account Brownian motion, or imperfections in the array, which will decrease sorting resolution. Qualitatively, the latter effect will be more pronounced for smaller particles with a diameter close to D_c, and low flow rates. Similarly, the influence of the shape and deformability of the particle on the critical diameter is not taken into account.

1. Davis, J. A. *Microfluidic Separation of Blood Components through Deterministic Lateral Displacement*. PhD thesis, Princeton University, (2008).

2. Comparison between the planar and 3D architecture

Reynolds number

We compared the 3D-DLD system presented in the manuscript (post diameter, d= 200 µm; centre to centre distance between posts, λ= 450 µm; gap between the posts, g= 250 µm and shift, s= 60 µm) and the 2D device with the identical parameters, except the height (here, 400 µm), which was corresponding to an aspect ratio 2, typical value for the planar systems. The velocity used for the calculations was derived from the flow rate inside of the 3D device 600 mL/min, recalculated based on the cross-section of the 2D and 3D device. The flow velocity in the 3D-DLD was 180 µm/s and 2500 µm/s for the planar device.

Hydraulic diameter for the 2D system was calculated using the height of the device (400 µm and the gap between the posts g= 250 µm). The post height for the 3D device is changing through the device; calculation was performed using the highest point of the device (7.5 mm), as this part of the device would be the first one affected by the transition between the laminar/ turbulent flow. Calculation of the Reynolds number were performed for the kinematic viscosity of the water at 20 °C ($1* 10^{-6}$ m^2/s).

Both systems were in the range of the laminar flow, with the Re number of the 3D device equal to 0.087 and being about ten times lower compared to the planar system with Re number equal to 0.77. Theoretically, the throughput of the device can be further increased up to the value of the Re = 10, leading to a flow rate of 1 mL/s inside the device.

Flow profile simulations

Flow simulations were performed using the COMSOL Multiphysics® platform involving laminar flow models. Fig S1a shows flow profiles of the planar and 3D-DLD design, without a significant difference between both architectures. Fig. S1b displays plotted velocity magnitudes from the area between the posts for both architectures. The design used for the simulations was identical to the design used for experiments.

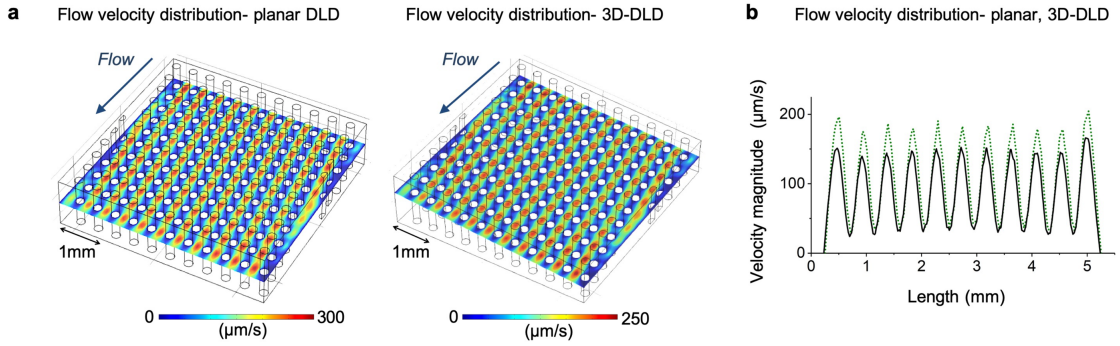

Fig. S1 a) Comparison of the flow velocity distribution inside the planar and 3D-DLD device. b) The flow velocity magnitude distribution in the middle of the gap area, perpendicular to the flow direction (planar design: green dotted line; 3D-DLD: black solid line).

Performed simulations revealed that the average minimal velocity and the average maximal velocity were 36 ± 3 μm/s and 182 ± 5 μm/s, respectively, for the planar design. Values for the 3D-DLD arrangement were comparable, with the average minimal velocity and average maximal velocities were 30 ± 3 μm/s and 147 ± 4 μm/s, respectively.

The particle travelling inside the device experiences flow between two concentric arches with a constant diameter and gap between them. The curvature of the posts is given by the outer dimensions of the centre element of the device i.e. 11 mm and 21 mm, respectively at the inner and outer arches of the sorting chamber. The curvature changes correspondingly of 2.3% for each two posts next to each other in the direction perpendicular to the flow. The particle travelling through the device would always have at least 100 times smaller radius in regards to the post curvature; based on the results from simulations, we were not expecting significant effect of the curvature on the flow velocity and trajectories of the particles travelling through the device. Due to the minimal difference between the planar and 3D-DLD systems, we estimated the value of the critical diameter using formula (Eq 1 above), as used for planar devices.

3. Characterization of the 3D-DLD cartridge

The homogeneity of the post's diameters within the 3D-DLD cartridge was studied using the partially printed arrays, with process stopped at 2, 4 and 6 mm (corresponding to 50, 100, 150 layers respectively, from the 237 total number layers per device: 25 using the DS-3000 resin and 212 made using DL-260). Characterization of the final post size inside the device was measured using the microscope TS-100 (Nikon). SEM images were obtained using a tabletop SEM microscope (TM3030 Hitachi Europe, France).

For each of these partially fabricated devices, we measured post diameters on five random posts in the lower, centre and upper part of the array. Results in figure S3 show the uniform and homogeneous distribution of the post diameters across the array. Measured cross-section area increased with the number of layers as expected due to the curvature of the posts (horizontal cut is larger than the post diameter). Detailed images of the array with the 100 printed layers can be seen in figure S3.

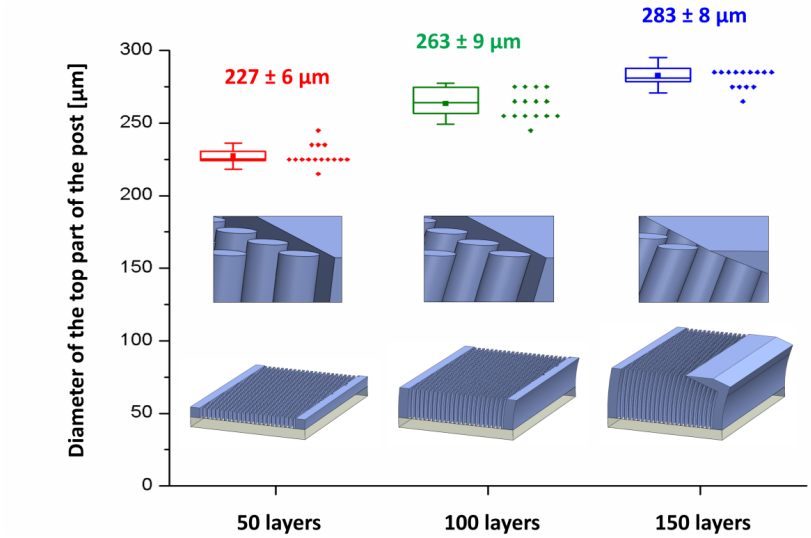

Fig. S2 Distribution of the post diameters across the array prepared partially with printed, 50, 100 and 150 layers. Insets show scheme of the device used for the measurement also with the details of the expected post shape at the horizontal cut where measurements were performed (mean value: square; median: line).

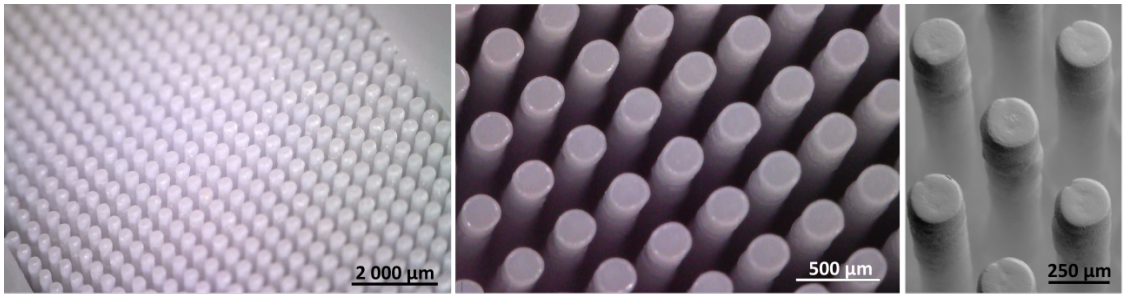

Fig. S3 Detailed pictures of the partially printed 3d-DLD cartridge. Properties of the array are the same as used for the particle sorting experiments: post diameter: 200 µm; centre to centre distance between posts: 450 µm and shift 60 µm.

4. Materials and methods:

All chemicals and materials were purchased in the analytical grade from Sigma Aldrich, if not stated otherwise.

Fabrication of the 3D-DLD system using stereo-lithography

All the parts fabricated using stereo-lithography (inlet, outlet, 3D-DLD sorting cartridge, observation window and a T-connector connecting reservoirs) were build using high-precision stereolithographic 3D printer 028J+ (working area: 90 x 90 x 90 mm, layer thickness: 10-100 μm, laser source: Solid State Budge - spot laser of ~20 μm, scanning method: galvanometer, scanning speed: 0 - 2200 mm s^{-1}) purchased from DWS. The individual parts were first designed using the Solidworks software (Dassault Systems SOLIDWORKS Corp.) and exported as .stl files. Designed parts were further processed using software provided together with the printer, Viscam (Marcam Engineering). The software is used to virtually slice designed parts into subsequent layers, and program laser trajectory to form these layers. Two materials were used, transparent DS-3000 and mechanically more stable, grey DL 260 (both, DWS).

Stereolithographic fabrication process (Fig. S4a) involves polymerization of the photo-curable material using a focused laser beam, precisely positioned by galvanometer-controlled mirrors. Photosensitive material is placed inside a resin tank, between the laser beam and the building platform. Distance between the building platform and the bottom of the resin tank defines the thickness of one slice, layer. Laser follows the path given by the cross-section of the structure to be produced. Solidified resin remains attached to the building platform and once the whole layer is completed, the platform moves up in the z-direction in the 10-100 μm steps, defining the resolution of the printer for the single layer. Resolution on X, Y plane is given by the size of the laser beam (~ 20 μm) and the control software, which predefines the laser path. Before starting to build the following layer, building platform moves again inside the resin tank to the position one slice thickness higher, compared to the previous position. The whole process continues until the entire part is built.

Standard process, described above does not allow prepare parts using a combination of the different materials; therefore, we optimised the protocol in order to implement a transparent wall in the designed 3D-DLD cartridge. Altered protocol is described in Fig. S4b. Compare to the standard process, design of transparent wall and enclosed array of pillars were prepared as separate files and also separately processed into slices and laser trajectories. However, it is important that two designs are at the matching position relative to the building platform, what was possible to be done at the Viscam software.

Transparent part, rectangular wall (1 x 12 x 60 mm) was printed first, using the optically transparent DS3000 resin. The slice thickness was 40 μm, contour was formed by two laser passes with 10 μm distance and the filling grid was printed with 40 μm distance between the consecutive laser paths.

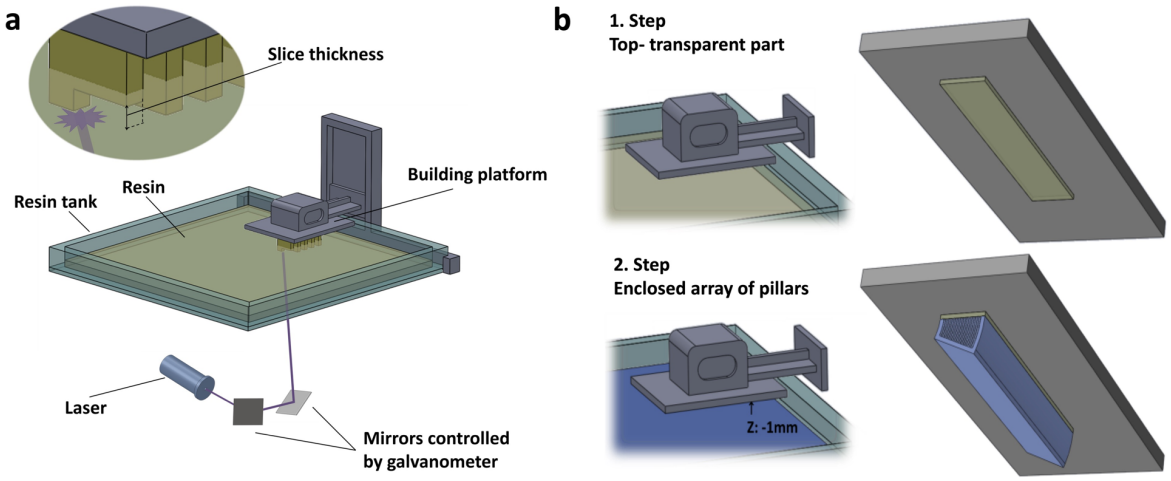

Fig. S4 Overview of the standard and optimized stereo-lithographic fabrication procedure. a) The standard stereo-lithography process: The photosensitive resin is polymerised by the laser beam, copying cross-section of the fabricating part. This process is repeated in a layer by layer manner until the whole part is formed. Between each layer-slice, building platform moves upwards, allowing liquid polymer to be renewed underneath it and returns to the position which is higher of a value of a slice thickness compare to the previous position.

b) Optimized protocol for the fabrication of multi-material device: first, using the transparent material, sidewall of the 3D-DLD cartridge is printed and well cleaned of the residual polymer. Following, zero position of the building platform is adjusted and the resin tank is exchanged for the second material. Figures on right shows view on the building platform with the printed structures. Both parts need to be printed at the same position at the building platform to be connected.

Before printing of the second part, the resin tank was exchanged for the tank holding the second, mechanically more stable material (DL 260). Building a platform with the printed part still attached was removed from the printer and cleaned from residual transparent resin using isopropanol and compressed air. Cleaned and dried platform was again placed inside the instrument and the relative zero position (distance between the position of the building platform and position at the bottom of the reservoir) is adjusted to take into the account height of the structure already printed on the building platform, in this case: 1mm.

Standard protocol involves printing of the first 5 layers in 20x lower laser speed (100 mm s^{-1}) to promote attachment of the polymerised resin on the building platform. This option had to be disabled since posts printed with the low laser velocity would have a significantly larger diameter than designed. The attachment of pillars to the transparent material was sufficient and no delamination was observed. The second part was formed using 40 µm slice thickness; contour was formed by three laser passes with 10 µm distances between trajectories and 30 µm distance for the filling grid. Fully printed cartridge was removed from the building platform, to ensure proper cleaning from the un-polymerised resin; cartridge was placed in the centrifugation tube (50 mL) with the approximately 30 mL of isopropanol and washed using the vortex mixer. Residual Isopropanol was removed from the cartridge using pressurized air stream and the cleaning process was repeated 3-4 times until resin was fully removed.

Finally, to improve transparency of the top part, small portion of the un-polymerised resin is deposited over the outer surface, pressed against a flat PE transparent foil and polymerised in

the UV oven (~ 60 s). This process allows removing pattern which is transferred to the printed part from the surface of the building platform.

Inlet and outlet parts were fabricated from DL 260 material, using 50 µm slice thickness and standard SLA process. Contour of each layer was made by three laser passes with 10 µm distance; filling grid was printed with 30 µm distance between the consecutive laser paths. Final parts were removed from the building platform and cleaned from un-polymerized resin using isopropanol and pressurized air stream. In the last step, parts were placed in a UV curing unit (model S2, DWS) for 40 minutes in order to finalize the polymerization process. Cleaning and UV curing steps are identical for all the components prepared using stereo-lithography.

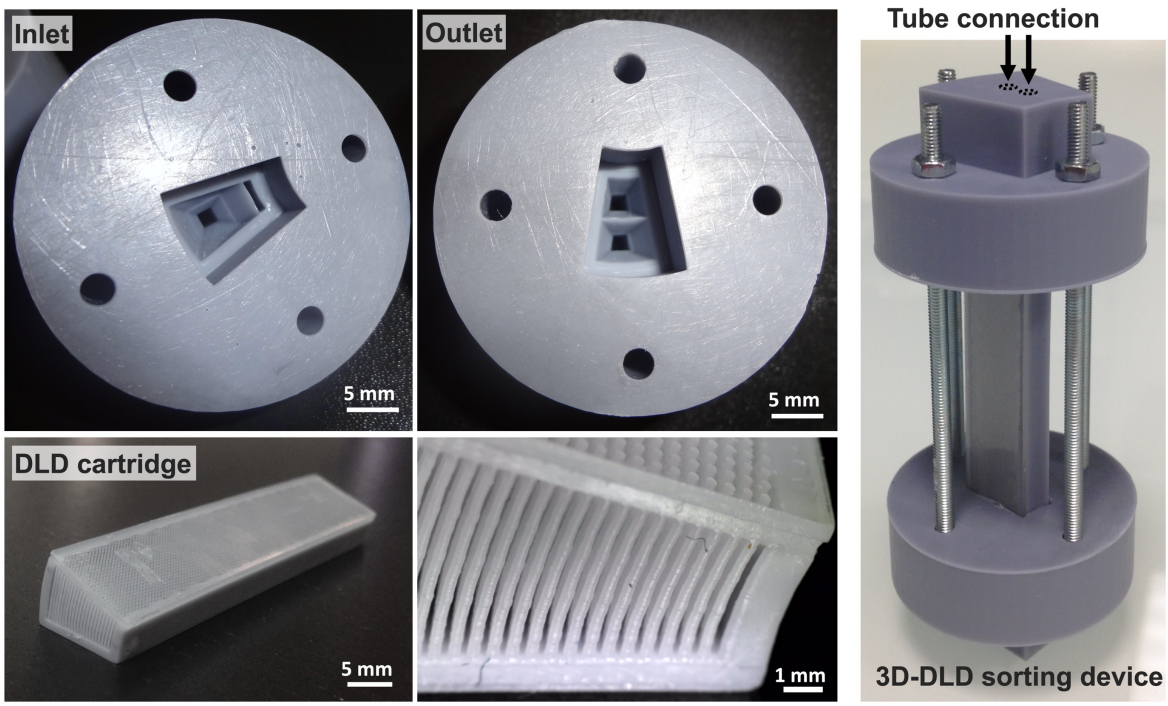

Fig. S5 Photographs of the inlet, outlet, 3D-DLD cartridge and the integrated fluidic cartridge system. Photographs of individual components and the integrated system with all parts connected using 4 standard 8 cm long screws with silicone glue applied at the connections to prevent leakage.

Observation of the particles after passing through the 3D-DLD sorting device was allowed using the observation window prepared by stereo-lithography as well. Window contained two square-shaped, (1.5 x 1.5 mm with length 30 mm) open channels (distance between channels: 1 mm) connected to the device outlets with the tubing. Whole part was printed using 50 µm slice thickness from the DS-3000 material using previously described parameters. Final part was enclosed using the SealPlate® film under the pressure 125 kg for 60s.

T-connector separating flow between the sample and the carrier fluid, composed of three connected channels (diameter: 2.4 mm) was fabricated using DS-3000 resin using the same parameters as observation window.

Experimental setup

In operation, the device was placed in a holder in up-right position, to avoid sedimentation of the sorted particles. The scheme showing the experimental setup with the connection to the fluidic and pressure channels is provided in Fig. S6. The integrated 3D-DLD system was connected to three separate reservoirs, two reservoirs with large volume (50 mL) containing the carrier fluid, and to one small reservoir (2 mL) used to supply the sample with mixes of particles. An additional reservoir with carrier fluid was added in order to push a small volume of the sample (1 mL) through the device (inner volume of the DLD cartridge ~1.5 mL) during priming of the device, in order to avoid unneeded sample loss. We used a T junction and two solenoid pinch valves to direct the flow either from the sample or from the carrier fluid reservoir towards the sample injection inlet (when dead volume is not an issue, e.g. for large volume samples, this part of the experimental setup can be removed). For samples with a small volume typically 1 mL and below, this approach allowed for the injection of several samples subsequently without interrupting the flow. The volume of the sample reservoir can be freely changed depending on the application.

Flow within the device was controlled by a pressure control unit, MFCS (Fluigent) with two flowmeters (range 0±1 mL/min) placed before each inlet channel to control and keep flowrate in both inlets stable and equal. Based on the selected flowrates, MFCS software adjusted pressure needed to achieve and maintain these two flowrates constant.

All experiments were performed at an adjusted flow rate 300 μL min^{-1} at both inlets. It is important to notice that the concentration of the particles injected to the system is limited by the used flowmeters. Passing of the beads through the flowmeter (measurement based on the heat transfer) causes a small disturbance in the measured value, which can still be compensated up to a certain level. This limitation can be in future avoided flow meter for a higher range of flow rates or syringe pumps.

Observation and quantification of the particles leaving through the outlets from the device were achieved using a separate observation chamber, and an ROIs encompassing a full cross-section of each channel was recorder by a USB camera. Particles passing through both channels of the observation chamber were quantified. The time resolution of the camera represented the main limitation of the flow rate for our experiments, but since there is no significant effect of the flow rate on the sorting resolution (up to Re =10) we selected the in-line quantification as a better tool to perform fundamental studies and optimization of the 3D-DLD system with the direct observation of the particle sorting.

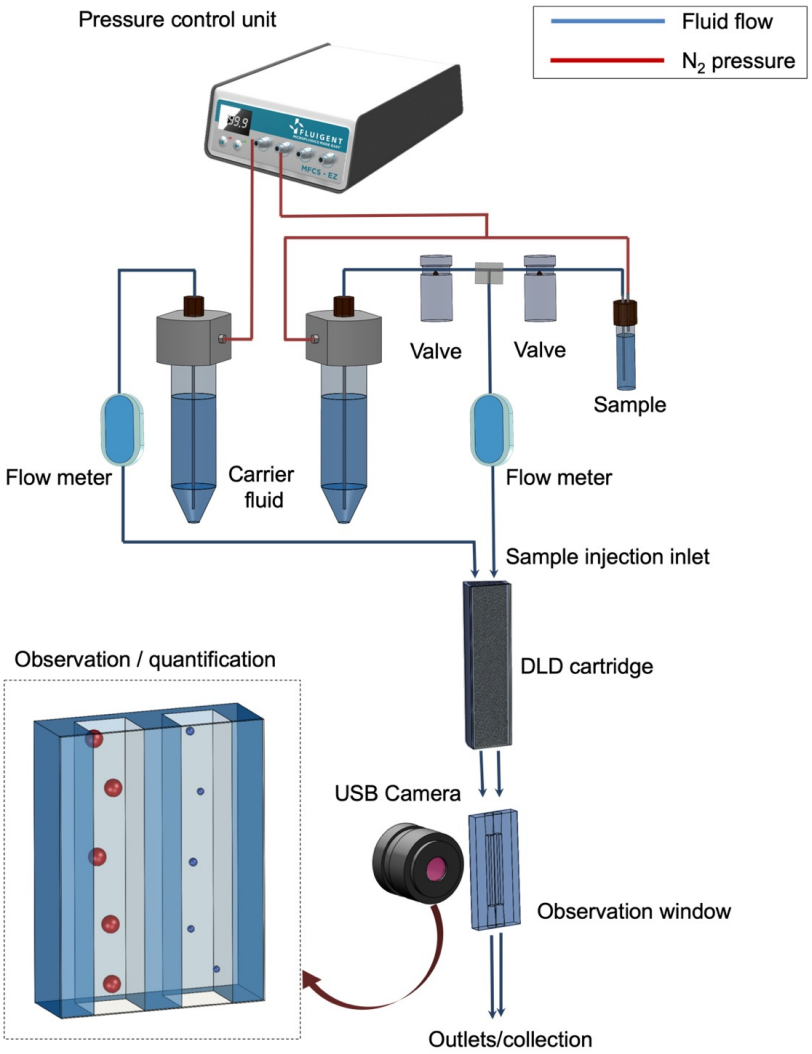

Fig. S6 Schematic representation of the experimental setup. Fluid flow inside the device (pictured only as DLD cartridge for simplification) was precisely controlled using pressure, with value adjusted and controlled by the two flowmeters placed before each of the inlets to the device. The first inlet (exterior side of the chamber regarding curvature) was used to supply carrier fluid, the second (interior side of the chamber regarding curvature) was used for sample injection. Switching between the two reservoirs was realized using two solenoid valves. Similarly, a T-junction on the pressure line allows to selectively push liquid from the sample reservoir, or a second reservoir containing carrier fluid. This design allows to reduce loss of precious sample (e.g. during device priming), or exchange between different samples without interruption of the flow. Fluids leaving the device pass through a secondary observation chamber, with an incorporated observation window equipped with a USB camera for particles tracking and counting. Inset (black frame) shows detail of the particles in channels as it was recorded by the camera and further used for the quantification.

Particle separation using 3D- DLD cartridge system

The 3D-DLD device was tested using polystyrene beads, with the diameter below and over the critical diameter estimated from the main value diameter of the posts inside the device. NIST traceable polystyrene size standard particles with 60 μm, 100 μm, 125 μm and 150 μm diameters (1% solids suspensions) were all obtained from Polysciences Europe GmbH.

Fluid flow inside the device was controlled using MFCS-8C (Fluigent) allowing to apply different pressures ranging from 0 to 25 mbar at each inlet. Pressure was regulated with two L-size flow units (range 0±1 mL min^{-1}) adjusting the pressure value to achieve an identical flow rate in both inlet channels, 300 μL min^{-1}.

Reservoirs for the carrier fluid (DI water supplemented with 1% Tween 20) were constructed using 50 mL centrifuge tubes connected to the pressure source through a Fluiwell (Fluigent) support. Reservoir for the particle mixture with 2mL volume was positioned above the chip to prevent sedimentation of the beads in the tubing. Outlet reservoirs were identical to reservoirs with the carrier fluid, collecting particles from two different outlets to the 50 mL tubes connected to the pressure source using Fluiwell system as well. Pressure control on the outlets was applied only to fill the whole device with the carrier fluid prior to the experiment.

Connection between the reservoirs and the device was enablable through the Tygon (ID: 0.8 mm; OD: 2.4 mm; purchased from VWR) and PTFE tubing (ID: 0.5 mm; OD: 1 mm, purchased from Sigma Aldrich). Selection between the reservoir with sample/carrier fluid was realized manually by switching between two solenoid pinch valves (only one valve was open during the device operation).

Particle suspension was prepared by pipetting beads from the stock solution in the 1 mL of the carrier fluid, with the volume as follows: 60μm beads (20 μL of the stock solution), 100μm beads (50 μL of the stock solution), 125 μm beads (60 μL of the stock solution) and finally for 150 μm beads (80 μL of the stock solution). Sample with the mixture of two different beads was prepared by pipetting 40 μL (100 μm beads) and 80 μL (150 μm beads) into 1 mL of the carrier fluid. Sample with the mixture of particles was agitated (lab dancer; VWR) shorty before switching of the valves and injecting to the system, to avoid sedimentation of the beads.

Observation during the experiments was done using a Dino Eye 5 Mp camera (Dino-Lite).

Fit of a Q function to the particles distribution data

The separation data plotted as a function of mean particles size (Fig. 3a main manuscript) was fitted with a Q-function (for particles in outlet 1 and its complement to 1, the cumulative distribution function, CDF) using Matlab software. The Q-function represents the probability that a random variable y (with variance σ and center X) is larger than x. In our case, the random variable is the position of the "cut-off" size between outlet 1 and outlet 2, X is the actual value, and x is the size of a given particle in the sorted pool. Applying this model thus assumes that the distribution of "trajectories" (combining all broadening effects, e.g. imperfections of the array, size distribution of the particles, Brownian motion, sedimentation) is a Gaussian. We believe that this assumption is reasonable, and it thus provides a lower-bound to the separation power of our actual system (understanding that since the breadth of the distribution in particles sizes also integrates a convolution by the distribution of sizes of the separated particles in each batch, and thus the absolute separation power for ideal particles would be better).

Thanks to the direct relationship between Q function and CDF, all data in outlets 1 and 2 could be fitted simultaneous with the same set of parameters to increase statistical power, by taking the complement to one of outlet 2 data. We also included in the fit the separation data obtained with mixed particles (Fig. 3c main manuscript).

A first fit was achieved using the function:

$F = 1 - (1 - \mathrm{erf}(a * (x - D_c)/\mathrm{sqrt}\,(2)))/2$

where x is the particles nominal size and a and D_c are left floating. This yields a = 0.1395 μm^{-1} i.e a σ value of = 7.2 μm, or a mean error relative to D_c of 5.4% , with a best fit D_c= 131.4 μm. This is close to the theoretical value 133 (the theoretical value is within the 95% probability interval of the fitted distribution: [129.4; 133.4]. As an additional test for consistency, we also performed the fit imposing D_c =133μm. In that case, σ is only moderately increased to 8.4 μm (relative mean error of 6.3%).

5. Discussion on clogging and recovery rate

Visual observation and long-term operation of the device suggest that the DLD array itself essentially did not trap particles in our experiments. It should be noted, however, that regarding the recovery rate of a full instrument, sedimentation in the connection tubes and reservoirs could lead to more significant issues rather than clogging within the device. In this first work on the technology, we focused on the fundamental aspects of particle sorting, and our system was not well adapted to study recovery globally and quantitatively, for two reasons: for better accuracy we studied separation "on flight" in a permanent regime, and do not take into account particles collection in transient regimes. Second, we did not particularly optimize connections towards recovery. In other words, our prototype was thought as a means for fundamental mechanistic studies, and not as a pre-industrial prototype. Finally, we also note that recovery rate and clogging strongly depend on the type of objects to be sorted, and could be of more importance for "soft" objects and notably living cells, than for PS particles. We thus believe that this will remain a question to investigate in a future more application-oriented study.